



## Friction stir welding of copper: Processing and multi-objective optimization

Gurmeet Singh<sup>a,b\*</sup>, Ankit Thakur<sup>b</sup>, Satpal Singh<sup>a,c</sup> & Neeraj Sharma<sup>d</sup>

<sup>a</sup>Thapar Institute of Engineering & Technology (Deemed University), Patiala 147004, Punjab, India

<sup>b</sup>Dr. B. R. Ambedkar National Institute of Technology, Jalandhar 144011, Punjab, India

<sup>c</sup>Design Engineer, Industrial Electric Mfg(IEM), BC V4W 3W7, Canada

<sup>d</sup>Maharishi Markandeshwar Deemed University, Mullana 133207, Haryana, India

Received:25 January 2019 ; Accepted:30 December 2019

Non-ferrous metals are difficult to weld as compared to the ferrous metals. Copper is one of the non-ferrous metals using worldwide in different manufacturing and other metal processing industries. This paper focuses on the processing of copper under friction stir welding (FSW) and the study of mechanical properties of friction stir welded (FSWed) copper joints. Different parameters of FSW have been studied with the help of  $L_9$  orthogonal array (OA). Rotational speed and traverse speed of the tool with three different tool materials have undergone for the parametric optimization. Tensile strength and impact strength have been optimized using the grey relational method. Results show a significant effect of parameters on responses. Finally, it has been concluded that the grey relational method is a robust method to optimize the combined set of responses in a single attempt. From results, it has been observed that the higher rotational speed and lower traverse speed with H13 tool material give better results for mechanical properties. Analysis of variance (ANOVA) has been used to find the percentage contribution of each parameter on mechanical properties. P-value has been found less than 0.05 which shows that the effect of each selected parameter on the result is significant. Microstructure study has been performed on scanning electron microscopy (SEM) and the change in grain size within the weld zone has been observed.

**Keywords:** Friction stir welding, Copper, Grey relational analysis, ANOVA, Tensile strength, Impact strength

### 1 Introduction

Copper is widely used in all electrical components due to its easy availability and high conductivity. All refrigeration and air-condition industries also use copper as a major component. Joining of copper is a necessary action for its better use in the above-said industry<sup>1-3</sup>. Retaining the mechanical properties during welding is the latest challenge for the researchers. FSW is the latest technique to develop sound weld for non-ferrous metals<sup>4-7</sup>. In FSW, as implied by its name, the friction and stirring play a vital role in this technique. Friction between a stirring tool and a work piece generates heat that helps to recrystallize the metal grains and allow freezing them as a joint<sup>8-9</sup>. This shows that the FSW is a solid-state welding technique. The schematic flow process of FSW is shown in Fig. 1. Rotating tool generates the heat while coming in contact with the metal piece and force them to get weld as a single piece as shown in the schematic flow process in Fig. 1. Development of FSW started in the late 90's and came into existence in 1991 at "The Welding Institute", UK<sup>10</sup>. This is recently developed technique as compared to the other

conventional welding techniques. Ericsson and Sandstrom<sup>11</sup> compared the mechanical strength of FSWed joints with tungsten inert gas (TIG) and metal inert gas (MIG) welding at their respective optimized set of parameters for AA6082. From comparative results, it was found that FSWed joints show higher strength under static and dynamic loading. TIG weld joints show better fatigue results than MIG weld joints. Yan *et al.*<sup>12</sup> studied the MIG welding and FSW of the Al-Zn AA specimen. Results prove that the FSW give higher hardness and tensile strength as compared to the MIG welding. Tensile strength of the specimens made using FSW is around 7% higher than those made using MIG welding. Gori and Verma<sup>13</sup> also conducted an experimental comparison of MIG and FSW on AA5083. As the results expected that the FSW show its edge on the conventional MIG welding and shows better hardness, fatigue, and tensile strength. From these researches, FSW sets a benchmark to get high mechanical properties. FSW was initially used for aluminium and its alloys only<sup>14</sup> but later it was also used for dissimilar metals<sup>15</sup>, other non-ferrous and ferrous metals as well. Welding of copper using FSW was done by a limited number of researchers<sup>16-18</sup>.

\*Corresponding author (E-mail: gurmeet.singh@thapar.edu)

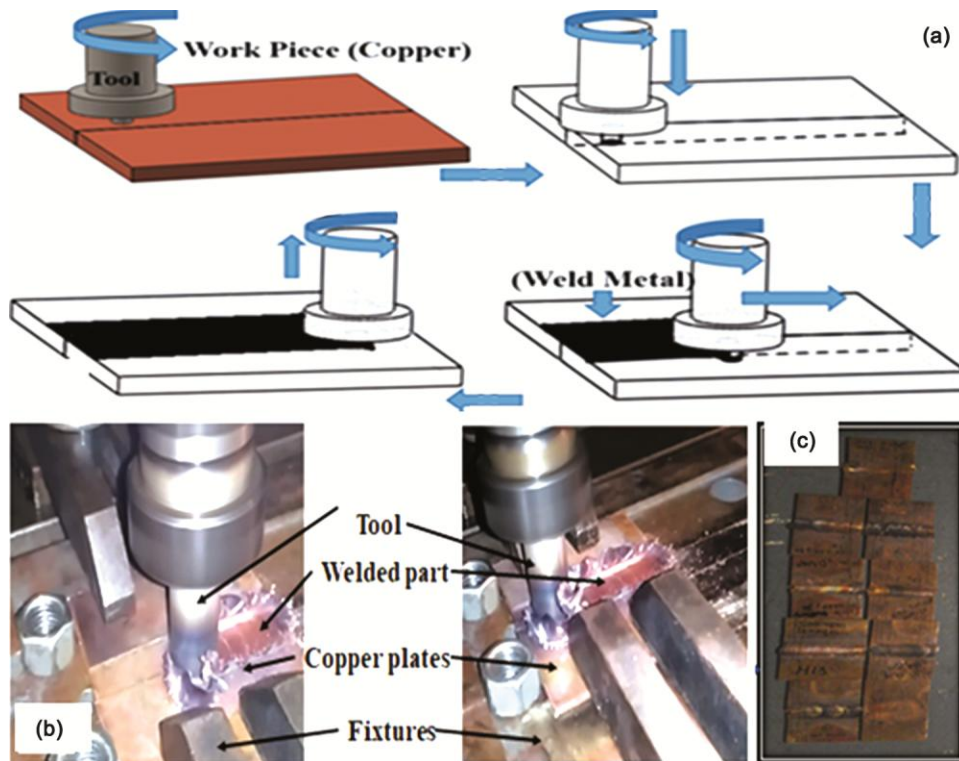


Fig. 1 — (a) Schematic flow process of FSW, (b) Experimentation process and (C) Welded specimen.

Sanusi *et al.*<sup>17</sup> performed friction stir spot welding on commercially used pure copper. From results, it was evident that the RS of the tool is an influential factor on mechanical properties. EDS and XRD results show that FSWed joints are more corrosion resistant. Kumar *et al.*<sup>18</sup> observed that the speed of rotation of a tool and its traverse play a vital role in the strength of the FSWed joints. Higher travel speed decreases the strength while higher tool rotation speed increases the mechanical properties within the selected range of parameters.

Taking in consideration the available research, it is clear that the researchers have done a little attempt on FSW of copper<sup>16-18</sup>. Hence, this article focuses on the parametric study and optimization of parameters for the welding of copper using FSW. Mechanical strength (tensile and impact) of the welded specimens are examined and multi-objective optimization of the parameter is performed using the grey-relational method.

## 2 Methodology and Experimentation

For experimentation, commercially used copper is arranged from market and cut in suitable pieces. The composition of material is checked through spectroscopy and found it is 99% copper. Three tools are

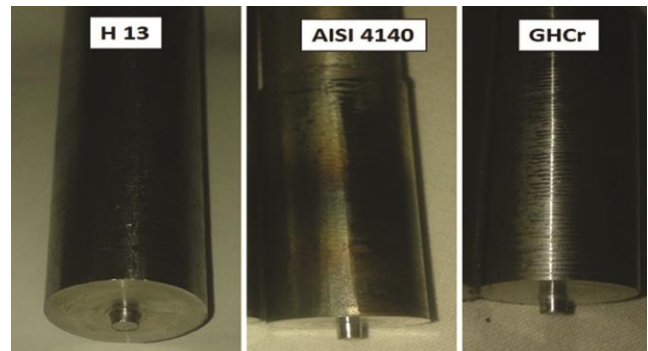


Fig. 2 — Tool fabricated for FSW.

fabricated using three different materials with different hardness at brinell scale; Grey cast iron (GHCr)(120HB), AISI 4140(197HB) and H13(513HB). Materials for tools are chosen on the basis of their mechanical properties because they all have high hardness and high recrystallization temperature than copper. Some previous researches also used these material as a tool for FSW of copper. Tools fabricated by these materials are shown in Fig. 2 along with the detailed drawing.

These fabricated tools are used as a parameter in optimization along with rotational speed and traverse speed of the tool. Parameters investigated in this study are shown in Table 1. On the basis of  $L_9$  orthogonal

Table 1 — Participating parameters and their levels for FSW.

Sr. No.	Parameter/Unit	Level 1	Level 2	Level 3
1	Rotational Speed (A) (rpm)	1200	2500	4000
2	Transverse Speed (B) (mm/min)	10	30	50
3	Tool Material (C)	GHCr	AISI 4140	H13

Table 2 — Experimental combinations and response outputs.

Exp. No	Rotational Speed (A)	Traverse Speed (B)	Tool Material (C)	Tensile strength (kN/mm <sup>2</sup> )	Impact strength (J)
1	1200	10	GHCr	0.171	200.695
2	1200	30	AISI4140	0.17	192.803
3	1200	50	H13	0.178	191.675
4	2500	10	AISI4140	0.186	198.44
5	2500	30	H13	0.202	216.48
6	2500	50	GHCr	0.176	209.715
7	4000	10	H13	0.212	227.755
8	4000	30	GHCr	0.192	239.03
9	4000	50	AISI4140	0.193	217.608

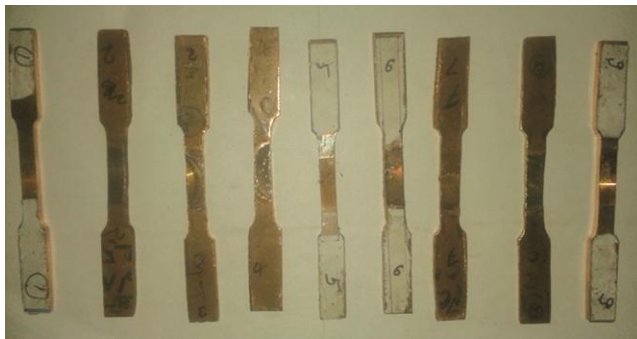


Fig. 3 — Samples prepared for testing.

array, total 9 experiments have been performed with different sets of parameters. The details of experimentation combination are shown in Table 2.

Welding has been performed on a vertical milling machine using fabricated tool fixed in the collet at the place of the cutting tool. The material is to be welded is fixed on the bed with abutting sides of plates. There is no need to prepare edges in this case as required in other conventional welding techniques. It is clear from the Fig. 1 that the tool rotates at a desired RPM and plunges within the material at the abutting edge first. This action develops some heat and because of this heat, welding at that edge starts. Now, the tool starts to travel along the edges and metal gets welded. At the end of the weld joint, there is an exit hole on the weld line. Specimens are cut from these 9 welded samples as per ASTM standards for tensile strength and impact strength tests. Specimens are prepared and shown in Fig. 3. All 9 specimens are tested using the universal testing machine for tensile test and impact

testing machine for impact strength. Tensile strength (kN/mm<sup>2</sup>) and impact strength (J) are recorded and listed in Table 2.

Effect of each parameter on the individual response is shown in the contour plots in Fig. 4. Each individual output shows its variation with change in input parameters. Plot (A) in Fig. 4 shows the variation in tensile strength with a change in the speed of the welding tool (both rotational and traverse). From contour plot (A) it can be seen that with an increase in rotational speed of the tool, tensile strength of the joint increases. On the other hand, increasing traverse speed results in less tensile strength. So from this plot, it can be said that the low traverse speed and high rotational speed give better mechanical strength to the welded joint. However, it can be observed from the plot that only high rotational speed does not give better results until it will get correlated by lower traverse speed as it is observed in the plot (A). Plot (B) shows the effect of rotational speed and type of tool on traverse speed. From this plot, it is evident that H13 tool material gives better tensile strength when using it with high rotational speed. Plot (B) also shows the significance of the variation of tool material as a parameter in this study. From plot (C) of Fig. 5, again it is clear that the H13 tool gives better tensile strength with low rotational speed only. From the plot (A, B & C) it is clear that high rotational speed, low traverse speed of the tool with the H13 tool will give the maximum tensile strength.

For impact strength, plot (D) shows change in impact strength with variation in traverse speed of the tool. It is clear that increasing rotational speed is also a dominating factor here. Increasing rotational speed indicates better impact strength of weld joint and variation in traverse speed of tool gives significant changes. For lower rotational speed, increasing traverse speed does not show any change on impact strength. However, from 2500 RPM, there is a vital variation in impact strength with variation in traverse speed. From plot, it is evident that traverse speed around 30 to 40 mm/min gives better impact strength with higher rotational speed within the selected parameter range. Plot (E) gives a description of the variation of impact strength with a change of rotational speed and tool material. It can be seen that H13 tool material is also a dominating factor as compared to other tool material. However, GHCr tool is also showing its importance with high rotational speed. Plot

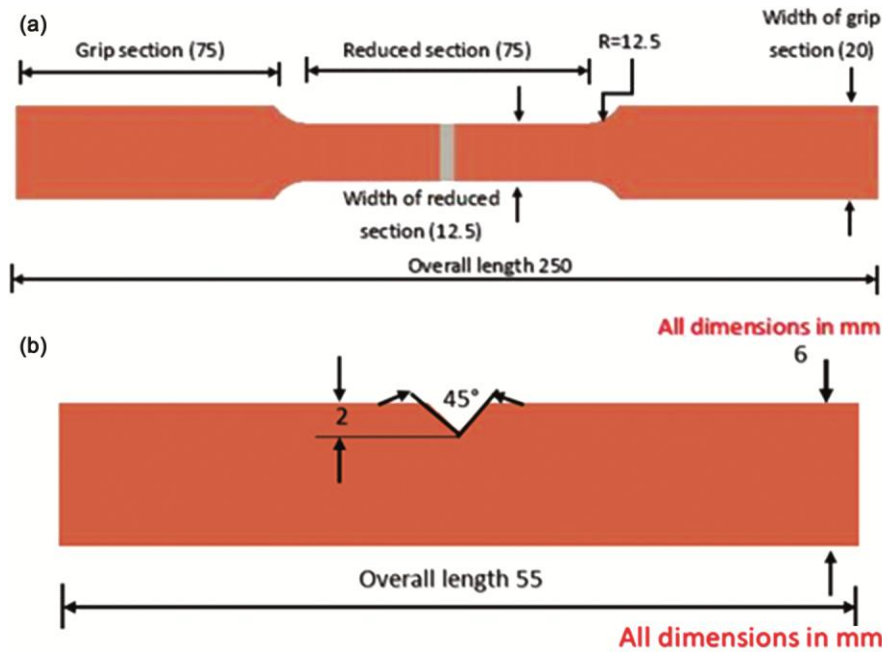


Fig. 4 — Detail drawing of specimen prepared for (a) Tensile testing and (b) Impact testing.

(F), presenting the variation of traverse speed and type of tool. From plot F, the effect of material with traverse speed is not clear. Although, H13 again shows its dominance over other tool material and GHCr tool material is also showing its effect within the range.

From contour plots, the overall conclusion can be made, that in some aspects, the results are very clear for the output response. But some factors show the confusing status of the response factors. For the better mechanical property of a welding joint, the tensile strength and impact strength both must be better in a single attempt. The impact strength must not be ignored for better tensile strength only and vice-versa. So, both responses must be optimized as a single result output. Taguchi optimization technique is a well-known established method of optimization for a single response. But all real-life problems are possessing multi attributes and require multi-objective optimization. Grey relational method is one of the finest methods through which the multi-response factors are optimized as a single output factor. Further, in this study, results from the experimentation method are solved using the grey relational method (GRM) and acquired a single output as grey relational grade (GRG). This will be helpful to identify the best combination of parameters which will give better combined results for both the output at a single attempt.

### 3 Grey Relational Analysis

Single response optimization is already in practice and used in different studies<sup>19-22</sup>. The present study emphasizes the use of multi-objective optimization. This is due to the fact that in real time problem, every joint will face different kinds of loading condition at a time. So the results of experimental data from Table 2 are undergone for further analysis. Tensile strength and impact strength values of individual experiments shown in Table 2 used to solve the multi-objective parametric optimization using GRM. It is already in use for multi-objective parametric optimization<sup>23-29</sup>. Results obtained during tensile and impact testing has been used to get the normalized value of the individual result. The formula used to get normalized values is shown in Equation 1, as high tensile and impact strength are desired for better results in welding and corresponding normalized values obtained using this are shown in Table 3. In the next step, this normalized value converted into grey relational coefficient (GRC) using equation 2 shown in Table 3. This will help to convert a complex system into simple and partial known information. Average value of GRC of both responses for a respective set of experiment is the GRG using Equation (3). A higher value of GRG is the optimum level for the multi-objective response of targeted mechanical properties<sup>23-29</sup>.



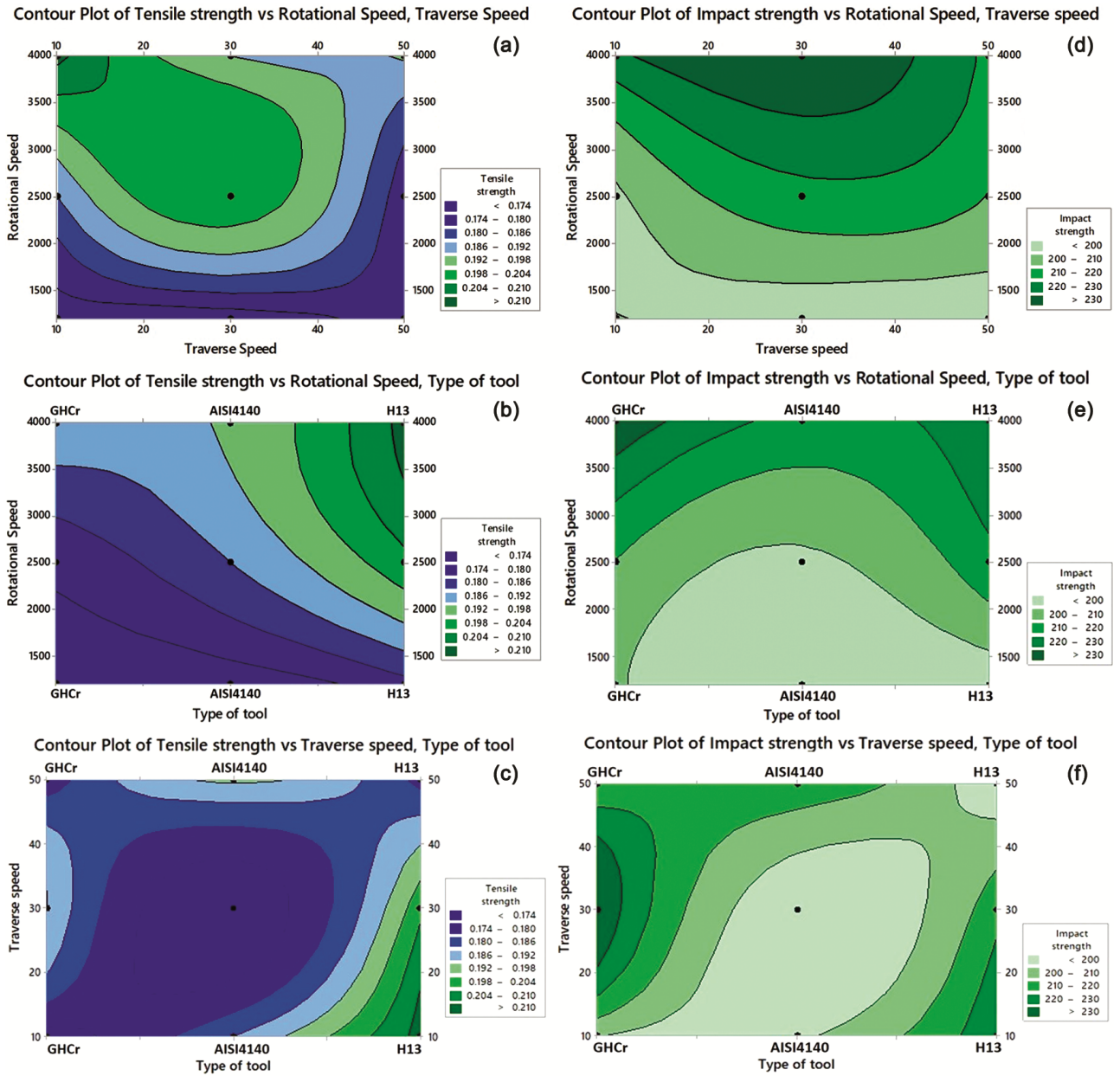


Fig. 5 — Contour plots showing the effects of parameters on individual outputs.

Table 3 — Normalized value, GRC and rank.

Exp. no.	Normalized value $\{xi(k)\}$		GRC $\{\xi i(k)\}$		$(GRG)\{\psi_g\}$	Rank
	Tensile strength	Impact strength	Tensile strength	Impact strength		
1	0.02381	0.190476	0.33871	0.381818	0.360264	7
2	0	0.02382	0.333333	0.338712	0.336023	9
3	0.190476	0	0.381818	0.333333	0.357576	8
4	0.380952	0.142857	0.446809	0.368421	0.407615	6
5	0.761905	0.52381	0.677419	0.512195	0.594807	3
6	0.142857	0.380952	0.368421	0.446809	0.407615	5
7	1	0.761905	1	0.677419	0.83871	1
8	0.52381	1	0.512195	1	0.756098	2
9	0.547619	0.54763	0.525	0.525006	0.525003	4

$$xi(k) = \frac{yi(k) - \min yi(k)}{\max yi(k) - \min yi(k)} \dots (1)$$

Here:  $xi(k)$  is the calculated normalized value.  $yi(k)$  is the respective value of response for that particular set of experiment.  $\max yi(k)$  and  $\min yi(k)$  is the maximum and minimum value obtained in the experimental results.

The formula used for grey relational coefficient (GRC) is

$$\xi = 0.5 / (1 - xi(k) + 0.5) \dots (2)$$

Here,  $\xi$  is the calculated GRC value for each individual value of normalized value ( $xi(k)$ ) using equation 2. GRC for tensile and impact strength calculated is shown in Table 4.

The formula used to calculate the GRG is

$$\Psi_g = 1/n \sum_{i=1}^n \xi i(k) \dots (3)$$

Here,  $\Psi_g$  is the calculated value for GRG for in the individual experiment.  $\xi i(k)$  is the grey relational Coefficient for tensile strength and impact strength and  $n$  is no of output responses.

**4 ANOVA**

ANOVA is performed on the GRG and statistically proves the effect of each parameter on the combined effect of results. Rotational speed of the tool

Table 4 — ANOVA for mean of GRG.

Parameters	SS	DOF	Variance	P-value	% age contribution
Rotational Speed (A)	0.1963	2	0.0981	0.009	72.03
Traverse Speed (B)	0.0293	2	0.0146	0.05	10.75
Tool Material (C)	0.0455	2	0.0227	0.03	16.69
Residual Error	0.0017	2	0.000		0.62

\*SS: sum of squares; DOF: degree of freedom

Table 5 — Response table for GRG.

Parameter	Level 1	Level 2	Level 3	Rank
Rotational Speed(A)	0.3531	0.4700	0.7066	1
Traverse speed(B)	0.5355	0.5623	0.4301	3
Tool Material (C)	0.4229	0.5080	0.5970	2

Table 6 — Conformation table.

	Optimized process parameters		
	Predicted value	Experimental value	Error Range
Optimal combination GRG	A3B1C3 0.8466	A3B1C3 0.8387	± 0.0079

shows the most of contribution on the output (72.03%). Percentage contribution of error is very less (0.62%) which shows the significance of the selection of parameters and their levels. The p-value for each participating parameters is below 0.05 which is also highly appreciable for the success of any statistical solution. Effect of each parameter and percentage contribution is described in the ANOVA Table 5.

**5 Confirmation of Results**

The confirmation test was performed to verify the results of grey relational analysis. The predicted value can be calculated using Eq. (4)<sup>25,29-30</sup>.

$$\Psi_p = \alpha_{0m} + \sum_{i=1}^k (\alpha_{0i} - \alpha_{0m}) \dots (4)$$

$$\Psi_p = 0.5093 + (0.7066 - 0.5093) + (0.5623 - 0.5093) + (0.5970 - 0.5093) \Psi_p = 0.8466$$

Here,  $\Psi_p$  is the estimated value of GRG.

$\alpha_{0m}$  is the mean value of total GRG calculated as in Table 6 for each experimentation condition.  $\alpha_{0i}$  is the mean value of GRG for the optimize combination of parameter and  $k$  is the number of total parameters involve in experimentation.

**6 Micro structural Study**

Welded specimen of FSW is undergone to SEM and the results from SEM images are helpful to understand the change in microstructure within the area of the welding zone. Comparative statement of SEM images is shown in Figs. 6. From these images, it is clearly evident that there is transformation of a microstructure while welding the copper using FSW. The base metal shows wide grain size in the microstructure image while weld zone of FSW of copper shows a fine grain size of the microstructure. The base metal of copper has grain size of more than 50  $\mu\text{m}$  while in weld zone average grain size is almost less than 20  $\mu\text{m}$ . The reason behind this fine grain structure is the dynamic blending of material while stringing the tool and allowing recrystallizing the metal at room temperature which gives a fine microstructure.

**7 Discussion**

The effect of welding parameters on welding strength, studied in this paper is clearly evident from the statistical analysis. From analysis based on experimental results, it is found that high rotational speed, moderate feed rate and H13 tool should be used. At high rotational speed, there is an accurate

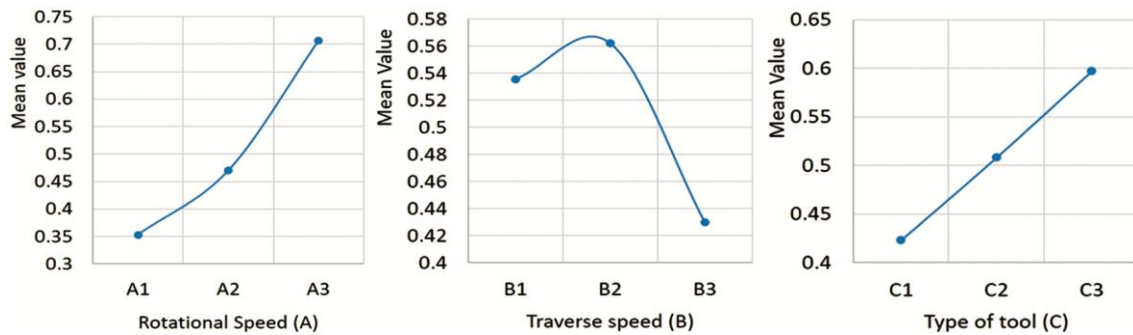


Fig. 6 — Graphs showing the variation of combined mechanical properties (tensile & impact strength) with different levels of parameters.

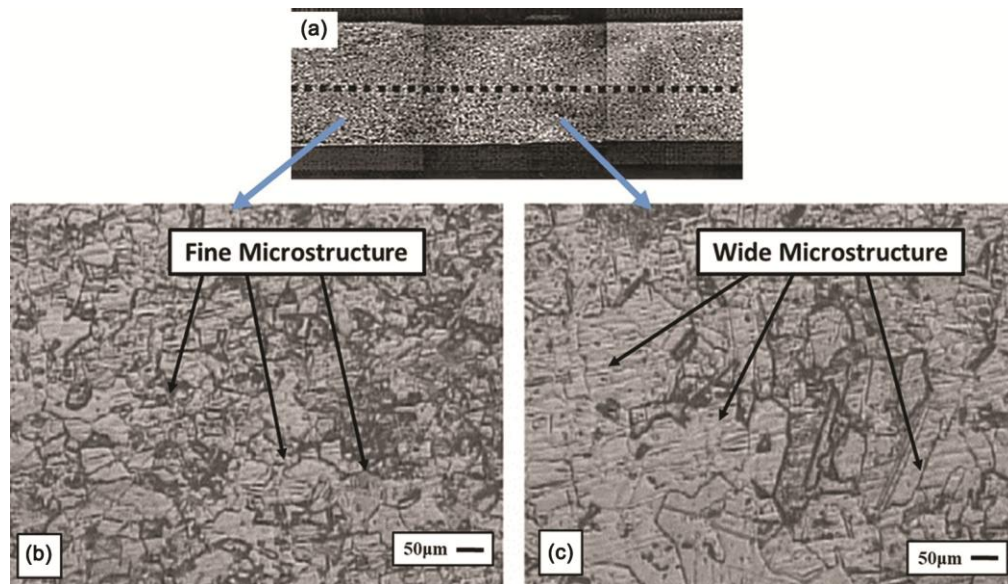


Fig. 7 — Scanning electron microscopy (a) Macroscopic image of welded specimen (b) Microstructure of weld zone and (c) Microstructure of base metal.

plastic deformation result as better grain refinement leads to the better bond strength between the grains<sup>6,8,14,15,19,31</sup>. For traverse speed of tool, the better results come up with the moderate traverse speed of tool. The reason for this kind of result is, at low traverse speed the displacement of material with in the stirring zone is not in uniform result as tunnel defect in weld zone. Whereas, at high traverse speed, material does not get enough time to get it homogenize and result as cavity in weld zone<sup>11,15,19,32,33</sup>. For tool material, material having high hardness shows the better mechanical strength. Higher hardness gives high coefficient of friction ( $\mu$ ) at the intermediate surface of tool and work material. Material with coefficient of friction ( $\mu$ ) produces high heat and a better plastic deformation<sup>34</sup>.

## 8 Conclusions

The study presents the use of grey relational method to optimize the FSW process parameters as

the combined effect of two response in a single step. The result shows that the optimization using GRM is very successful because the error range in predicted and experimental value is very low ( $\pm 0.0079$ ). The key points of the result are as below:

- (i) The analysis of grey relational method shows that the rotational speed of 4000 rpm with lowest travel speed 10 mm/min and H13 tool gives better result in term of mechanical properties of the welded joint.
- (ii) Rotational speed shows its highest contribution (72.03%) on the multiple responses in term of mechanical properties followed by tool material (16.69%) and traverse speed (10.75%) as evident from ANOVA.
- (iii) From confirmation test, it is proved that the grey relational method is perfectly suitable for optimization the multiple responses for FSW.
- (iv) The technique used will simplify the complex process and can do multi-objective optimization

and directly applicable to the safety of the structure and other component made by FSW of copper.

- (v) The microstructure study has been performed using SEM and shows that with FSW the weld zone has a uniform and fine microstructure as compared to the base metal, which shows the annealing effect within the weld zone.

## References

- 1 Fattah-alhosseini A, Taheri A H & Keshavarz M K, *Transac Indian Institute Met*, 69 (2016) 1423.
- 2 Nia A A & Ali S A, *Metall Mater*, 23 (2016) 799.
- 3 Pashazadeh H, Teimournezhad J & Masoumi A, *Int J Adv Manuf Technol*, 88 (2017) 1961.
- 4 Azizi A, Barenji R V, Barenji A V & Hashemipour M, *Int J Adv Manuf Technol*, 86 (2016) 1985.
- 5 Sakthivel T & Mukhopadhyay J, *J Mater Sci*, 42 (2007) 8126.
- 6 Mehta K P & Badheka V J, *Mater Manuf Process*, 31 (2016) 233.
- 7 Sinhmar S & Dwivedi D K, *Mater Sci Eng: A*, 684 (2017) 413.
- 8 Mishra R S, De P S & Kumar N, *Friction Stir Welding and Processing*, Science and Engineering, (Springer International Publishing: Switzerland), 2014.
- 9 Dragatogiannis D A, Koumoulos E P, Kartsonakis I, Pantelis D I, Karakizis P N & Charitidis C A, *Mater Manuf Process*, 31 (2016) 2101.
- 10 Thomas W, Friction stir butt welding, International Patent Application No. PCT/GB92/0220 1991.
- 11 Ericsson M & Sandstrom R, *Int J Fatigue*, 25 (2003) 1379.
- 12 Sinhmar S & Dwivedi D K, *Corrosion Sci*, 133 (2018) 25.
- 13 Gori Y & Verma R P, *J Graphic Era University*, 5 (2012) 10.
- 14 Jangra K K, Sharma N, Khanna R & Matta D, *Proc Institution Mech Eng, Part L: J Mater: Des Appl*, 230 (2016) 454.
- 15 Jain S, Sharma N & Gupta R, *Eng Solid Mechanics*, 6 (2018) 51.
- 16 Carlone P, Astarita A, Palazzo G S, Paradiso V & Squillace A, *Int J Adv Manuf Technol*, 79 (2015) 1109.
- 17 Sanusi K O, Akinlabi E T, Muzenda E & Akinlabi S A, *Mater Today: Proc*, 2 (2015) 1157.
- 18 Kumar P, Singh S, Singh G & Dua A, *IOSR J Mech Civil Eng*, 16 (2016) 65.
- 19 Senthilraja R & Sait A N, *Mater Sci*, 51 (2015) 180.
- 20 Shojaeefard M H, Akbari M, Khalkhali A, Asadi P & Parivar A H, *Mater Des*, 64 (2014) 660.
- 21 Shojaeefard M H, Khalkhali A, Akbari M & Tahani M, *Mater Des*, 52 (2013) 587.
- 22 Singh G, Jain V, Gupta D & Ghai A, *J Mech Behavior Biomedical Mater*, 62 (2016) 355.
- 23 Deng J L, *J Grey Sys*, 1 (1989) 1.
- 24 Palanikumar K, Latha B, Senthilkumar V S & Paulo D J, *Mater Manuf Process*, 27 (2012) 297.
- 25 Meena V K & Azad M S, *Mater Manuf Process*, 27 (2012) 973.
- 26 Kumar A, Sharma S C & Beri N, *Mater Manuf Process*, 25 (2010) 1041.
- 27 Singh S, *Int J Adv Manuf Technol*, 63 (2012) 1191.
- 28 Tang L & Yang S, *The Int J Adv Manuf Technol*, 67 (2013) 2909.
- 29 Singh G, Jain V & Gupta D, *Proc Institution Mech Engs, Part H: J Eng Med*, 231 (2017) 1133.
- 30 Lin Z C & Ho C Y, *Int J Adv Manuf Technol*, 21 (2003) 10.
- 31 Sinhmar S & Dwivedi D K, *J Manuf Process*, 37 (2019) 305.
- 32 Abrahams R, Mikhail J & Fasihi P, *Mater Sci Eng: A*, 751 (2019) 363.
- 33 Verma, J, Taiwade R V & Reddy C, *Mater Manuf Process*, 33 (2018) 308.
- 34 Padmanaban G & Balasubramanian V, *Mater Des*, 30 (2009) 2647.